ChemComm

RSC Publishing

COMMUNICATION

View Article Online
View Journal | View Issue

Cite this: *Chem. Commun.*, 2013, **49**, 3016

Received 24th January 2013,
Accepted 26th February 2013

DOI: 10.1039/c3cc40630j

www.rsc.org/chemcomm

In vivo imaging using polymeric nanoparticles stained with near-infrared chemiluminescent and fluorescent squaraine catenane endoperoxide†

Jung-Jae Lee, Alexander G. White, Douglas R. Rice and Bradley D. Smith*

Polystyrene nanoparticles stained with squaraine catenane endoperoxide exhibit remarkably high chemiluminescence and enable optical imaging of biodistribution in living mice. Whole-body chemiluminescence imaging was much more effective than fluorescence at identifying lung accumulation of the nanoparticles.

The widespread introduction of relatively cheap, technically-straightforward, optical imaging stations has made it possible to incorporate small animal optical imaging into mainstream biomedical research and drug discovery programs.[1] Planar optical imaging of small animals is amenable to longitudinal and high throughput studies because images can be recorded rapidly, using harmless near-infrared light, and multiple animals can be imaged simultaneously.[2] Whole-body images can be acquired in either; (a) fluorescence mode, which typically involves illumination of the entire living animal to achieve excitation of targeted or activated fluorescent probes, or (b) chemiluminescence mode, which usually employs genetically modified cells expressing luciferase enzymes that consume chemical fuel and produce light.[3] A common drawback with both optical modalities is limited penetration of the light through skin and tissue, a problem that is minimized by employing wavelengths in the window of 650–900 nm. We are pursuing a new optical molecular imaging method using small polymeric particles that incorporate synthetic dyes that we call CLF dyes because they are simultaneously chemiluminescent and fluorescent. Unlike, inorganic nanoparticles with persistent luminescence,[4] the chemiluminescence with CLF dyes is thermally-activated (that is, no chemical or electrical stimulus is needed) which means that the dyes can be stored at low temperature and they only become self-illuminating when warmed to body temperature.

This current study compares two types of related CLF dyes; recently described Squaraine Rotaxane Endoperoxide (**SREP**),[5] and previously unreported Squaraine Catenane Endoperoxide (**SCEP**) (Fig. 1). They are interlocked molecules with two components, a macrocyclic endoperoxide that is the primary energy source for the chemiluminescence, and an encapsulated fluorescent squaraine chromophore. We have previously shown that **SREPs** undergo a thermally-activated cycloreversion reaction that releases excited-state singlet oxygen and emits 733 nm light.[6] The chemiluminescence apparently comes from the encapsulated squaraine chromophore after energy transfer from the released singlet oxygen.[7] The flux of singlet oxygen that is produced by this thermal process is quite low and **SREPs** are not toxic to cells.[8] A preliminary, highly controlled study of **SREP**-stained microparticles simply injected at different depths into mouse leg muscle (the microparticles did not enter the animal's systemic circulation and were imaged immediately after injection) indicated that target signal contrast with fluorescence imaging was

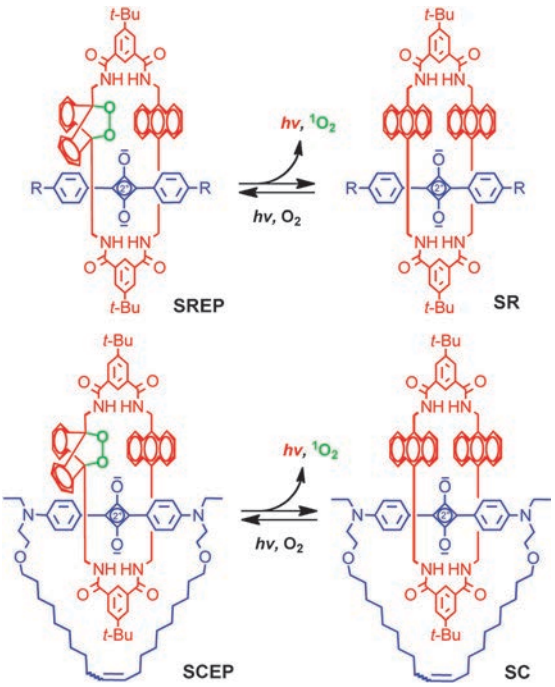

Fig. 1 Thermal cycloreversion of **SREP** or **SCEP** releases singlet oxygen and emits near-infrared light. The reverse process of light irradiation in the presence of air is employed to prepare the storable endoperoxide compounds.

Department of Chemistry and Biochemistry, University of Notre Dame, Notre Dame, IN 46556, USA. E-mail: smith.115@nd.edu; Fax: +1 574 6316652; Tel: +1 574 6318632

† Electronic supplementary information (ESI) available: Experimental details and additional information. See DOI: 10.1039/c3cc40630j

much more "surface weighted" than chemiluminescence imaging. With superficial target sites (<2 mm deep), fluorescence imaging produced the highest Target-to-Background Ratio (TBR). But TBR for fluorescence imaging quickly dropped towards unity with increasing tissue depth due to increased contribution of the background signal.[9] With chemiluminescence imaging, the attenuation of TBR with tissue depth was more linear and gradual, such that chemiluminescence imaging produced the highest TBR in deeper target sites. *These results suggest a new paradigm for optical molecular imaging using nanoparticle probes containing these CLF dyes. First, high contrast chemiluminescence imaging is employed to locate the probe in vivo at relatively deep target sites and then there is a switch to fluorescent mode for subsequent microscopic studies of thin biopsy or histopathology sections taken from the exact same specimen*. A necessary requirement for further development of this imaging paradigm is the production of nanoparticle probes with very high chemiluminescence intensity. Here, we report that **SCEP**-stained carboxylate-functionalized polystyrene nanoparticles exhibit substantially more chemiluminescence intensity than analogous **SREP**-nanoparticles. We utilize this crucial technical breakthrough to directly compare the capabilities of whole-body fluorescence and chemiluminescence imaging to track systemic biodistribution of polymeric nanoparticles in a living mouse after intravenous injection. The work has relevance in nanomedicine since small polymeric particles are used clinically as embolization agents,[10] and they are under active preclinical investigation as pulmonary drug delivery vehicles,[11] *in vivo* imaging probes,[12] and adjuvants for vaccination.[13]

The synthesis of **SREP** has been reported before, and the same photoxidation method was employed to make **SCEP**. That is, simple irradiation of the known parent squaraine catenane (**SC**)[14] with red light in the presence of air produced **SCEP** cleanly and in essentially quantitative yield with no evidence of over oxidation. In organic solution, the chemical and photophysical properties of **SCEP** and **SREP** are very similar. They both can be stored at −20 °C until needed and upon warming they undergo chemiluminescent cycloreversion reactions that hardly change the fluorescence profile of the encapsulated squaraine dye. The cycloreversion processes were conveniently monitored by the changes in ^{1}H NMR spectra, and the first-order rate constant for **SCEP** cycloreversion (k_1 = 0.39 h^{-1}, $t_{1/2}$ = 1.8 h) was found to be roughly two times faster than **SREP** (k_1 = 0.17 h^{-1}, $t_{1/2}$ = 4.0 h) at 38 °C in $C_2D_2Cl_4$. In each case, standard chemical trapping experiments showed that almost two thirds of the released oxygen was excited state singlet oxygen (see ESI†). A straightforward particle-swelling procedure was employed to stain 20 nm carboxylate-functionalized polystyrene nanoparticles with **SREP** or **SCEP** at 4 °C.[5] In both cases, equally high loadings of fluorescent nanoparticles were obtained, but chemiluminescence intensity with the **SREP**-nanoparticles was disappointingly low. In comparison, the **SCEP**-nanoparticles emitted thirty-fold higher chemiluminescence, a key discovery that permitted the mouse imaging studies described below.‡ Shown in Fig. 2 are representative chemiluminescent and fluorescent pixel intensity images of a vial, containing an aqueous dispersion of **SCEP**-nanoparticles, that was warmed from 4 °C to 38 °C. As expected, both the chemiluminescence and the fluorescence signals were observed selectively

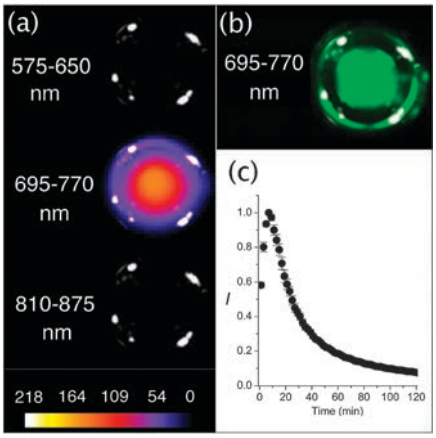

Fig. 2 (a) Chemiluminescence pixel intensity maps of a vial at 38 °C containing an aqueous dispersion of **SCEP**-nanoparticles (20 nm carboxylate-functionalized polystyrene) and emitting only in the 695–770 nm channel of the imaging station. (b) The same vial emitted strong fluorescence in the 695–770 nm channel. (c) Chemiluminescence decay profile of the vial.

in the 695–770 nm emission filter channel. The chemiluminescence signal became more intense over the first few minutes as the cycloreversion rate increased with warming; subsequently, the emission decayed exponentially with a detectable signal persisting beyond two hours. The integrity of the dye-stained nanoparticles under physiological conditions was evaluated by *in vitro* experiments that incubated the particles with red blood cells and looked for transfer of the dye to the cells (see ESI†). Essentially no dye uptake was observed over 45 minutes suggesting that significant leakage of **SCEP** from the nanoparticles was unlikely to occur over the shorter time required for *in vivo* mouse imaging studies.

Fig. 3a shows the results of a typical whole-body imaging experiment with chemiluminescence and fluorescence pixel intensity maps of an anesthetized mouse at 10 minutes after tail vein injection of **SCEP**-nanoparticles (20 nm carboxylate-functionalized polystyrene). The TBR for each image was calculated by dividing the mean pixel intensity of the target lung region (T) by the mean pixel intensity of a non-target background region (B). Even a cursory inspection of the chemiluminescence and fluorescence images reveals that they are quite different. Although the chemiluminescence mean pixel intensity is substantially weaker, the average TBR for each lung is 6.3 ± 0.3 (N = 3) and more than double the average lung fluorescence TBR of 2.7 ± 0.3 (N = 3). Furthermore, the chemiluminescence image suggests that most of the nanoparticles are in the lungs, whereas the fluorescence image indicates that the particles are primarily in the liver (Fig. 3b). *Ex vivo* analysis of the organs after animal sacrifice proved that most of the nanoparticles were indeed in the lungs (Fig. 3c). In other words, *in vivo* chemiluminescence imaging was substantially more accurate than *in vivo* fluorescence imaging. The fluorescence imaging is misleading because it is highly "surface weighted" – even though the liver contained fewer **SCEP**-nanoparticles, the liver is closer to the animal surface and produces a much brighter fluorescence signal compared to the lungs which are located more deeply in the thoracic cavity partly behind the heart. The superior *in vivo* quantification provided by chemiluminescence imaging, compared to fluorescence imaging,

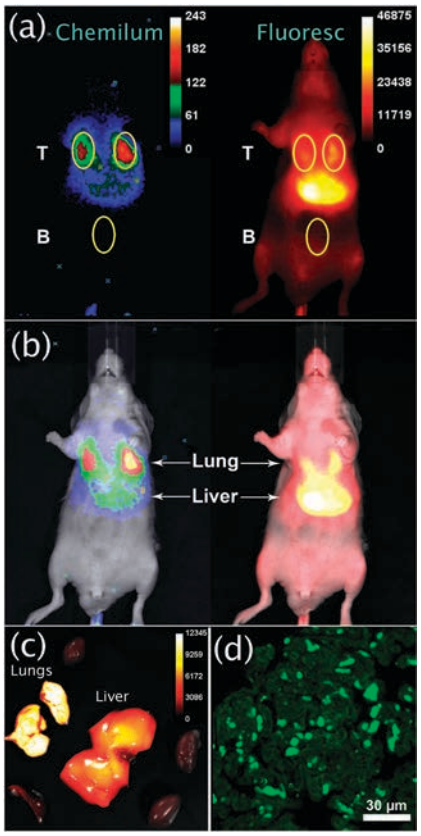

Fig. 3 (a) Ventral chemiluminescence and fluorescence pixel intensity images of an anesthetized mouse at 10 minutes after tail vein injection of **SCEP**-nanoparticles (20 nm carboxylate-functionalized polystyrene). (b) Overlay with bright field image highlights the different ratios of lung and liver signals. (c) *Ex vivo* fluorescence image of excised organs showing that most of the nanoparticles are in the lungs. (d) Fluorescence micrograph (695–770 nm emission channel) of lung histology section showing micrometer diameter aggregates of nanoparticles.

is mentioned occasionally in the imaging literature,[15] but the practical implications of this disparity have not previously been described. The whole-body images in Fig. 3b provide a striking demonstration of the difference in capabilities to accurately image deep-tissue sites. The direct comparison is enabled by the unique optical properties of **SCEP**-nanoparticles, which are both highly fluorescent and chemiluminescent.

Extensive lung retention of these 20 nm nanoparticles was not expected since the average diameter of mouse lung capillaries is 5.7 μm,[16] and several previous reports have shown unimpeded passage of micron-sized polymeric particles.[17] Shown in Fig. 3d is a fluorescent micrograph of a thin, histological section taken from excised lung tissue. The micrograph was acquired several days after the mouse was sacrificed, so the nanoparticles were no longer chemiluminescent but they were still highly fluorescent. The **SCEP** signal appears as micrometer-scale, fluorescent aggregates which is consistent with self-aggregation of the nanoparticles in lung capillaries after dosage;§ however, alternative explanations, such as nanoparticle uptake by lung epithelial cells, cannot be ruled out at this point. In any case, the results show clearly that chemiluminescence imaging can be employed to accurately identify lung accumulation in living mice. With further refinement we are hopeful that our optical imaging paradigm using CLF dyes can be utilized to monitor, in real-time, the progress of various types of lab animal experiments and nanoparticle delivery procedures.

This work was supported by the Notre Dame Integrated Imaging Facility and NIH grants R01GM059078 (B.D.S.) and T32GM075762 (D.R.R.). The animal studies were approved by the Notre Dame Institutional Advisory Care and Use Committee.

Notes and references

‡ Comparative control studies of micron-sized polystyrene particles, stained with either **SREP** or **SCEP**, showed very similar chemiluminescence intensities. We tentatively attribute the enhanced chemiluminescence observed with 20 nm **SCEP**-nanoparticles to the relatively compact and spherical molecular shape of **SCEP**. This might allow deeper penetration of the dye into the core of the highly curved nanoparticles, away from the surrounding quenching water, with a concomitant increase in energy transfer efficiency from the singlet oxygen released during the cycloreversion.
§ Dynamic light scattering studies showed that the **SCEP**-nanoparticles do not self-aggregate in the stock solution.

1 (*a*) G. D. Luker and K. E. Luker, *J. Nucl. Med.*, 2008, **49**, 1; (*b*) M. Baker, *Nature*, 2010, **463**, 977.
2 (*a*) J. L. Kovar, M. A. Simpson, A. Schutz-Geschwender and D. M. Olive, *Anal. Biochem.*, 2007, **367**, 1–12; (*b*) S. Mather, *Bioconjugate Chem.*, 2009, **20**, 631.
3 (*a*) *Chemiluminescence and Bioluminescence: Past, Present and Future*, ed. A. Roda, Royal Society of Chemistry, Cambridge, UK, 2010; (*b*) J. A. Prescher and C. H. Contag, *Curr. Opin. Chem. Biol.*, 2010, **14**, 80.
4 (*a*) Q. L. de Chermont, C. Chanéac, J. Seguin, F. Pellé, S. Maîtrejean, J. P. Jolivet, D. Gourier, M. Bessodes and D. Scherman, *Proc. Natl. Acad. Sci. U. S. A.*, 2007, **104**, 9266; (*b*) T. Maldiney, C. Richard, J. Seguin, N. Wattier, M. Bessodes and D. Scherman, *ACS Nano*, 2011, **5**, 854; (*c*) T. Maldiney, G. Sraiki, B. Viana, D. Gourier, C. Richard, D. Scherman, M. Bessodes, K. Van den Eeckhout, D. Poelman and P. F. Smet, *Opt. Mater. Express*, 2012, **2**, 261.
5 J. M. Baumes, J. J. Gassensmith, J. Giblin, J. J. Lee, A. G. White, W. J. Culligan, W. M. Leevy, M. Kuno and B. D. Smith, *Nat. Chem.*, 2010, **2**, 1025.
6 J. M. Baumes, I. Murgu, A. Oliver and B. D. Smith, *Org. Lett.*, 2010, **12**, 4980.
7 C. G. Collins, J. M. Baumes and B. D. Smith, *Chem. Commun.*, 2011, **47**, 12352.
8 J. J. Lee, A. Goncalves, B. Smith, R. Palumbo, A. G. White and B. D. Smith, *Aust. J. Chem.*, 2011, **64**, 604.
9 J. V. Frangioni, *Mol. Imaging*, 2009, **8**, 303.
10 R. López-Benítez, G. M. Richter, H. U. Kauczor, S. Stampfl, J. Kladeck, B. A. Radeleff, M. Neukamm and P. J. Hallscheidt, *Cardiovasc. Intervent. Radiol.*, 2009, **32**, 615.
11 (*a*) H. L. Kutscher, P. Y. Chao, M. Deshmukh, S. S. Rajan, Y. Singh, P. D. Hu, L. B. Joseph, S. Stein, D. L. Laskin and P. J. Sinko, *Int. J. Pharm.*, 2010, **402**, 64; (*b*) P. Y. Chao, M. Deshmukh, H. L. Kutscher, D. Y. Gao, S. S. Rajan, P. D. Hu, D. L. Laskin, S. Stein and P. J. Sinko, *Anticancer Drugs*, 2010, **21**, 65; (*c*) H. L. Kutscher, P. Chao, M. Deshmukh, Y. Singh, P. Hu, L. B. Joseph, D. C. Reimer, S. Stein, D. L. Laskin and P. J. Sinko, *J. Controlled Release*, 2010, **143**, 31; (*d*) B. D. Kurmi, J. Kayat, V. Gajbhiye, R. K. Tekade and N. K. Jain, *Expert Opin. Drug Delivery*, 2010, **7**, 781.
12 J. Napp, T. Behnke, L. Fischer, C. Wurth, M. Wottawa, D. M. Katschinski, F. Alves, U. Resch-Genger and M. Schäferling, *Anal. Chem.*, 2011, **83**, 9039.
13 (*a*) A. C. Rice-Ficht, A. M. Arenas-Gamboa, M. M. Kahl-McDonagh and T. A. Ficht, *Curr. Opin. Microbiol.*, 2010, **13**, 106; (*b*) F. Blank, P. Stumbles and C. von Garnier, *Expert Opin. Drug Delivery*, 2011, **8**, 547.
14 J. J. Lee, J. M. Baumes, R. D. Connell, A. G. Oliver and B. D. Smith, *Chem. Commun.*, 2011, **47**, 7188.
15 (*a*) T. Troy, D. Jekic-McMullen, L. Sambucetti and B. Rice, *Mol. Imaging*, 2004, **3**, 9; (*b*) K. M. Cui, X. Y. Xu, H. Zhao and S. T. C. Wong, *Luminescence*, 2007, **23**, 292.
16 (*a*) A. Geelhaar and E. R. Weibel, *Respir. Physiol.*, 1971, **11**, 354; (*b*) U. O. Häfeli, K. Saatchi, P. Elischer, R. Misri, M. Bokharaei, N. R. Labiris and B. Stoeber, *Biomacromolecules*, 2010, **11**, 561.
17 (*a*) T. Yamaoka, Y. Tabata and Y. Ikada, *J. Bioact. Compat. Polym.*, 1993, **8**, 220; (*b*) B. H. Simon, H. Y. Ando and P. K. Gupta, *J. Pharm. Sci.*, 1995, **84**, 1249; (*c*) Q. P. Gao, B. Hansen and R. Seljelid, *Drug Delivery*, 1997, **4**, 93; (*d*) L. Illum, S. S. Davis, C. G. Wilson, N. W. Thomas, M. Frier and J. G. Hardy, *Int. J. Pharm.*, 1982, **12**, 135.

